Near-infrared surface brightness fluctuations and optical colours of Magellanic star clusters

R. A. González-López-lira, M. Y. Albarrán, Mustapha Mouhcine, M. C. Liu, G. Bruzual-A., Bertrand de Batz

Mon. Not. R. Astron. Soc. **363,** 1279–1289 (2005) doi:10.1111/j.1365-2966.2005.09553.x

Near-infrared surface brightness fluctuations and optical colours of Magellanic star clusters

R. A. González-Lópezlira,[1⋆] M. Y. Albarrán,[1] M. Mouhcine,[2,3] M. C. Liu,[4]†
G. Bruzual-A.[5] and B. de Batz[6]

[1]*Centro de Radioastronomía y Astrofísica, Universidad Nacional Autónoma de México, Campus Morelia, Michoacán CP 58190, Mexico*
[2]*School of Physics and Astronomy, University of Nottingham, Nottingham NG7 2RD*
[3]*Observatoire Astronomique de Strasbourg (UMR 7550), 11, rue de l'Université, 67000 Strasbourg, France*
[4]*Institute for Astronomy, University of Hawaii, 2680 Woodlawn Drive, Honolulu, HI 96822, USA*
[5]*Centro de Investigaciones de Astronomía, Apartado Postal 264, Mérida 5101-A, Venezuela*
[6]*GEPI (CNRS UMR 8111), Observatoire de Paris, 5 place J. Janssen, 92195 Meudon Cedex, France*

Accepted 2005 August 13. Received 2005 July 27; in original form 2005 May 18

ABSTRACT

This work continues our efforts to calibrate model surface brightness fluctuation luminosities for the study of unresolved stellar populations, through a comparison with the data of Magellanic Cloud star clusters. We present here the relation between absolute K_s-band fluctuation magnitude and $(V–I)$ integrated colour, using data from the Two-Micron All-Sky Survey (2MASS) and the Deep Near-Infrared Southern Sky Survey (DENIS), and from the literature. We compare the star cluster sample with the sample of early-type galaxies and spiral bulges studied by Liu et al. We find that intermediate-age to old star clusters lie along a linear correlation with the same slope, within the errors, of that defined by the galaxies in the $\bar{M}_{K_s}$ versus $(V–I)$ diagram. While the calibration by Liu et al. was determined in the colour range $1.05 < (V–I_C)_0 < 1.25$, ours holds in the interval $-5 \gtrsim \bar{M}_{K_s} \gtrsim -9$, $0.3 \lesssim (V–I) \lesssim 1.25$. This implies, according to Bruzual–Charlot and Mouhcine–Lançon models, that the star clusters and the latest star formation bursts in the galaxies and bulges constitute an age sequence. At the same time, a slight offset between the galaxies and the star clusters [the latter are ∼0.7 mag fainter than the former at a given value of $(V–I)$], caused by the difference in metallicity of roughly a factor of 2, confirms that the $\bar{M}_{K_s}$ versus $(V–I)$ plane may contribute to break the age–metallicity degeneracy in intermediate-age and old stellar populations. The confrontation between models and galaxy data also suggests that galaxies with K_s fluctuation magnitudes that are brighter than predicted, given their $(V–I)$ colour, might be explained in part by longer lifetimes of thermally pulsing asymptotic giant branch stars. A preliminary comparison between the H 2MASS data of the Magellanic star clusters and the sample of 47 early-type galaxies and spiral bulges observed by Jensen et al. through the $F160W$ *Hubble Space Telescope* filter leads to the same basic conclusions: galaxies and star clusters lie along correlations with the same slope, and there is a slight offset between the star cluster sample and the galaxies, caused by their different metallicities. Magellanic star clusters are single populations, while galaxies are composite stellar systems; moreover, the objects analysed live in different environments. Therefore, our findings mean that the relationship between fluctuation magnitudes in the near-infrared, and $(V–I)$ might be a fairly robust tool for the study of stellar population ages and metallicities, could provide additional constraints on star formation histories, and aid in the calibration of near-infrared surface brightness fluctuations for cosmological distance measurements.

⋆E-mail: r.gonzalez@astrosmo.unam.mx
†Alfred P. Sloan Research Fellow.

Key words: stars: AGB and post-AGB – Magellanic Clouds – galaxies: star clusters – galaxies: stellar content – infrared: galaxies – infrared: stars.

1 INTRODUCTION

Whereas surface brightness fluctuation (SBF) measurements are now well established as very powerful distance indicators (e.g. Tonry, Ajhar & Luppino 1990; Tonry et al. 1997; Jensen et al. 2001, 2003; Liu & Graham 2001; Mei, Quinn & Silva 2001), their potential for the study of unresolved stellar populations, although recognized long since (Tonry & Schneider 1988; Tonry, Ajhar & Luppino 1990; Liu, Charlot & Graham 2000; Blakeslee, Vazdekis & Ajhar 2001; Jensen et al. 2003), has so far remained mostly unfulfilled. We have recently (González, Liu & Bruzual 2004, hereafter Paper I; González, Liu & Bruzual 2005; Mouhcine, González & Liu 2005) started an effort to calibrate near-infrared (near-IR) SBFs, mostly for their use as probes of the characteristics of stellar populations. The idea is to compare SBFs derived from single stellar population (SSP) models with observed fluctuation luminosities of Magellanic Cloud (MC) star clusters. Our contribution has been to build 'superclusters' with the data, in order to reduce the stochastic effects produced by the inadequate representation, in single star clusters, of the luminosity functions of stars going through short evolutionary phases (Santos & Frogel 1997; Bruzual 2002; Cerviño et al. 2002; Cantiello et al. 2003; Cerviño & Valls-Gabaud 2003; Paper I); i.e. the asymptotic giant branch (AGB) and upper red giant branch (RGB). Superclusters, first introduced in Paper I, are built by coadding MC clusters, in the compilation of van den Bergh (1981), that have the same SWB class (Searle, Wilkinson & Bagnuolo 1980). The SWB classification is based on two reddening-free parameters, derived from integrated *ugvr* photometry of 61 rich star clusters in the MCs. Later, Elson & Fall (1985) assigned SWB classes to 147 more clusters using *UBV* photometry.

The SWB ranking constitutes a smooth, one-dimensional sequence that Searle et al. interpreted as one of increasing age and decreasing metallicity; this interpretation is supported by stellar photometry and spectroscopy in individual clusters (e.g. references in Searle et al. 1980; Frogel, Mould & Blanco 1990). The sequence discovered by Searle and collaborators was arbitrarily segmented by them to define a classification with seven types of clusters; however, facts such as the apparently smooth progression in age and metallicity along the sequence, and the similarity between the handful of type VII MC clusters and the old and metal-poor halo globular clusters of the Milky Way have translated into the customary adoption of the working hypothesis that clusters within each SWB type have approximately the same stellar population.[1] In our case, as we have already explained in Paper I, binning the data into superclusters is the compromise we have found most convenient to adopt in order to try to circumvent the problem of small-number statistics posed by individual star clusters. We have devised eight superclusters, one for each of the seven different SWB classes, plus one 'pre-SWB-class' supercluster with the youngest objects in the sample.

[1] To give just a couple of examples, Cohen (1982) presents ages and metallicities of the seven SWB classes based on spectrophotometric data of a few stars within only a couple of clusters of each class; Frogel et al. (1990) do the same, based on near-IR photometry of 400 stars in and around 39 clusters.

In the present paper, we focus on the relationship between $\bar{M}_{K_s}$ and the $(V–I)$ colour. The merits of going to IR wavelengths have been discussed at length (e.g. Liu et al. 2000; Paper I; Mouhcine et al. 2005). Summarizing, the light of intermediate-age and old populations is dominated by bright and cool stars for which the spectral energy distributions peak in the near-IR, at the same time that dust extinction is reduced. On the other hand, there is a scarcity in the near-IR of both accurate empirical calibrations and self-consistent models, a fact that we hope we are contributing to remedy with our work.

In the particular case of the correlation between $\bar{M}_{K_s}$ and $(V–I)$, Liu et al. (2002) confirmed a linear dependence of $\bar{M}_{K_s}$ with $(V–I)$ in a sample of 26 ellipticals, S0s and spiral bulges in the Local Group, Fornax, Virgo, Eridanus and Leo. The relation had already been hinted at by the data set of Jensen, Tonry & Luppino (1998), which covered only half the range in colour [$\sim 1.16 < (V–I) < \sim 1.24$]; it was more clearly shown by Mei et al. (2001), mainly through the inclusion of data for NGC 4489 at $(V–I) \lesssim 1.05$. Liu et al. filled significantly the gap in colour with observations of Fornax objects. Probing the extent (in age, metallicity and, ultimately, environment) to which this relation remains valid has obvious implications for an accurate calibration of near-IR SBFs as distance indicators, and hence for a precise determination of H_0 through these measurements (see Liu et al. 2002 for a detailed discussion).

There are also implications of this correlation from the point of view of stellar population studies. Because, in general, observed properties of stellar populations are luminosity-weighted, and given that after $\sim$12 Myr the youngest stars are also the most luminous in the optical and near-IR wavelengths, the tendency uncovered by Liu et al. (2002) could be tracing the most recent burst of star formation in each of these systems. This is the conclusion reached in the cited work, after comparing their results with predictions by Liu et al. (2000) (based on the models that would later be published by Bruzual & Charlot 2003, hereafter BC03), Worthey (1993b) and Blakeslee Vazdekis & Ajhar (2001) (based on the Vazdekis et al. 1996 models). Although there are disagreements among such predictions (especially in the derived metallicities obtained, respectively, from the Liu et al. models on one hand, and from those of Blakeslee et al. on the other), all of them point toward a large spread in age for the sample, from less than 5 Gyr to more than 12 Gyr. Furthermore, in all three sets of models confronted by Liu et al. (2002), the age and metallicity sequences are not parallel in at least some regions of the $\bar{M}_{K_s}$ versus $(V–I)$ plane, opening the possibility of using it as a diagnostic for breaking the age–metallicity degeneracy.

This study of the relationship between $\bar{M}_{K_s}$ and $(V–I)$ in the MC star clusters is complementary in two advantageous ways to the investigation by Liu et al. (2002). First, because the superclusters are approximately single-age, single-metallicity stellar populations, the star formation bursts that they represent are not masked by an underlying population, as it occurs in galaxies; hence, they likely constitute a better set for comparison with simple stellar population models. Secondly, the MC clusters span an even larger extent in age, i.e. from a few $\times 10^6$ yr to $\sim 10^{10}$ yr, than that of the galaxies and bulges in the Liu et al. sample. Consequently, they cover a range

roughly three times larger in $\bar{M}_{K_s}$ and four times more extended in $(V–I)$.

For this investigation, we have made use of K_s-band data retrieved from the Two-Micron All-Sky Survey (2MASS; Skrutskie et al. 1997), $I_{\rm Gunn}$ (I_g or I henceforth) data from the Deep Near-Infrared Southern Sky Survey (DENIS; Epchtein et al. 1997) and V data from different sources in the literature. This paper is organized as follows. In Section 2, we give a brief summary of the data acquisition and characteristics, as well as of our own treatment of such data. In Section 3, we present the ingredients of the stellar population synthesis models, and a comparison between the two sets of models used here. In Section 4, we compare the theoretical predictions to the observations. Finally, in Section 5, the results of the present work are discussed and summarized.

2 OBSERVATIONAL DATA OF MAGELLANIC CLOUD STAR CLUSTERS

2.1 2MASS data

K_s data for 191 MC clusters from the compilation of van den Bergh (1981) and analysed by Elson & Fall (1985, 1988) were retrieved from the 2MASS archive. The data processing has been presented at length in Paper I. Succinctly, the fluctuation luminosity is the ratio of the second moment of the luminosity function ($\Sigma n_i L_i^2$) to its first moment (the integrated luminosity, $\Sigma n_i L_i$), as expressed by the equation:

$$\bar{L} \equiv \frac{\Sigma n_i L_i^2}{\Sigma n_i L_i}. \quad (1)$$

Bright stars are the main contributors to the numerator, whereas faint stars contribute significantly to the denominator. The second moment of the luminosity function was derived by measuring the flux of resolved, bright stars in the MC clusters, while the integrated luminosity was computed from the total light detected in the images, after removing the sky background emission. In order to reduce the stochastic errors produced by the small numbers of luminous and cool RGB and AGB stars in single star clusters, eight superclusters were assembled with the 2MASS data, one for each of the seven different SWB classes, plus one 'pre-SWB-class' supercluster; this was accomplished by stacking individual clusters with the same SWB type.[2] The mosaics were used to measure the integrated light of the superclusters. To derive the second moment of the luminosity function, star lists for each one of the superclusters were integrated with entries from the 2MASS Point Source Catalogue (PSC). The photometry of the point sources was performed by the 2MASS collaboration on individual cluster frames, previously to and independently from this work (i.e. we did not measure fluxes from point sources on the stacked supercluster frames), following the standard procedure of profile-fitting plus curve-of-growth aperture correction.[3] Because all near-IR zero-points were obtained in a uniform fashion, it is unlikely that they are an important source of systematic error.

As explained in Paper I, the quoted fluctuation errors include stochastic variations produced by small-number statistics. These were calculated following a statistical approach introduced by Buzzoni (1989) and Cerviño et al. (2002), based on the assumption that the variables involved have a Poissonian nature. In this framework, stochastic errors scale as $M_{\rm tot}^{-1/2}$, where $M_{\rm tot}$ is the total mass of the stellar population. We refer the reader to Appendix A for a short discussion on the subject of stochastic variations.

Besides the problem of small-number statistics, assessing crowding is crucial for accurate SBF measurements of star clusters. Through the blending of sources, crowding can in principle make the numerator of equation (1) larger and hence the SBF magnitude brighter. Another source of systematic error is the sky level, which impacts the denominator of equation (1). Both crowding and sky determination have been lengthily addressed in Paper I, and revisited in Mouhcine et al. (2005) to consider the corrected fluctuation measurements of superclusters type I and II (González et al. 2005). With regard to crowding, we did not follow there the usual procedure of analysing the effects of the addition of artificial stars on the measured fluctuations. Instead, we compared the fluctuations derived from annular regions of the superclusters (i.e. regions with diverse crowding properties), and checked whether the different regions would be deemed crowded by the criterion, developed by Ajhar & Tonry (1994), that the two brightest magnitudes of stars cover more than 2 per cent of the area. We also tested our hypothesis that the PSC quality flags would be very helpful to eliminate blended sources by obtaining, again in annuli, fluctuation values with and without stars with faulty photometry. While crowding affects preferentially the centres of clusters, errors in the sky subtraction will impact more the fainter, outer regions. Our analysis allowed us to determine that the circular regions within 1 arcmin of the centre of the superclusters provide the better balance of uncertainties owing to crowding and sky subtraction, at the same time that they are less vulnerable to stochastic effects than smaller annular regions. Consequently, for the SBF measurements we use only integrated light and point sources within 1 arcmin (at the distance of the LMC) from the centres of the superclusters. Just point sources with good photometry, according to the PSC quality flags,[4] were included. We adopted distance moduli of $(m - M)_o = 18.50 \pm 0.13$ to the LMC and $(m - M)_o = 18.99 \pm 0.05$ for the SMC (Ferrarese et al. 2000).

2.2 DENIS data

The observations for DENIS were carried out between 1995 and 2001, and in particular the MC data were taken between 1995 and 1998. Cioni et al. (2000) give a good summary of the DENIS instrument, and data acquisition and characteristics. The instrument was mounted at the Cassegrain focus of the 1-m European Southern Observatory (ESO) telescope at La Silla, Chile, and could obtain simultaneously images at I_g, J and K_s with three cameras. These had, respectively, a Tektronix CCD with 1024^2 pixels (each 1×1 arcsec^2), and two NICMOS infrared detectors with 256^2 pixels (each 3×3 arcsec^2, but the J and K_s exposures were dithered to a 1-arcsec pseudo-resolution). DENIS scanned the southern sky in strips of 30° in declination and 12 arcmin in right ascension. Each strip comprises 180 12×12 arcmin^2 images, with an overlap of 2 arcmin between every pair. The integration time at I is 9 s; at J and K_s, the integration time is 1 s, but each released image is made

[2] Individual cluster images were multiplicatively scaled to a common photometric zero-point (determined by the 2MASS team) and dereddened; Small Magellanic Cloud (SMC) clusters were geometrically magnified to place them at the distance of the Large Magellanic Cloud (LMC).

[3] See http://www.ipac.caltech.edu/2mass/releases/allsky/doc/sec4_4.html.

[4] See http://www.ipac.caltech.edu/2mass/releases/allsky/doc/sec1_6b.html#origphot.

Table 1. Clusters in Paper I not included in this paper.

Supercluster	Name	Reason
I	L 51	No available calibrated DENIS data
	SL 477	No available calibrated DENIS data
	NGC 1951	No available calibrated DENIS data
	NGC 1986	No available calibrated DENIS data
III	NGC 1953	No available calibrated DENIS data
V	NGC 1777	Two bright foreground stars
	NGC 2193	No available calibrated DENIS data

up of nine individual microscanned exposures, for a total integration time also of 9 s.

The nominal 5σ limiting magnitude at I is 18 mag, and the typical size of a detected point source is smaller than 2 arcsec FWHM. However, for this particular project we are concerned with the photometric accuracy at I achieved for extended sources. From those clusters for which more than one I calibrated exposure is available, we find the photometric error to be $\sim$0.1 mag.

Flattened and bias-subtracted I images that contain the Magellanic clusters in our sample were retrieved from the DENIS archive. The sample is the same one from which the $\bar{M}_{K_s}$ measurements were obtained, with the exception of seven clusters, presented in Table 1; there are no calibrated DENIS data for six of them, while the other one (NGC 1777) has two bright foreground stars and we do not know whether the V measurement has been duly corrected. Instrumental zero-points were obtained from the DENIS archive as well. Next, the I-band flux was derived for each cluster, in a diaphragm with the same size as that used for the corresponding V-band measurement. V magnitudes and diaphragms were taken from van den Bergh (1981), except for those clusters listed in Table 2.[5] It is worth noticing that, because we do not know the coordinates of the centres of the V observations, the derived $(V–I)$ colour could be slightly biased to the red.[6] The sky emission for each cluster was determined from an annulus separated from the photometric diaphragm by a buffer area; the best sizes of both buffer and sky annuli were chosen after visually inspecting the images, with the purpose of excluding from the sky measurements bright foreground stars and, most importantly, residual cluster light.

The individual cluster V- and I-band flux values were then corrected for extinction as in Paper I, Table 1, and averaged to obtain the V and I fluxes for the superclusters, and their $(V–I)$ colours. As before, when clusters do not have individually measured reddening, we have assumed $E(B–V) = 0.075$ for the LMC and $E(B–V) = 0.037$ for the SMC (Schlegel, Finkbeiner & Davis 1998). Once again, given that the extinction corrections of all the data (V, I and K_s) were done consistently by us, this is probably not an important source of systematic error. Absolute zero-points were taken, for V from Bessell (1979), and for I from Fouqué et al. (2000), who determined it especially for DENIS. The average $(V–I)$ colours of the superclusters (and, for completeness, also the $\bar{M}_{K_s}$ values derived in Paper I and in González et al. 2005) are presented in Table 3. The quoted errors in $(V–I)$ were derived as follows. The dispersion of I flux measurements was calculated for those clusters for which multiple images were available. For clusters with single images, the average dispersion was adopted. The error in I for the superclusters was found by adding the individual dispersions in quadrature, and then dividing by $(N-1)^{1/2}$, where N is the number of individual clusters in each supercluster. Finally, the error in $(V–I)$ was computed by assigning to the V value the same uncertainty as that for I, and assuming a correlation coefficient of 0.5 between V and I (see, for example, Cerviño et al. 2002; Paper I).[7] We note, however, that while we find an average dispersion at I of $\sim$0.1 mag for individual clusters, there might be systematics, such as flattening defects, that would increase this error. Indeed, Paturel et al. (2003) give an average uncertainty of $\sim$0.2 mag at I for their measurements of galaxy magnitudes. We also remark that the dispersion of $(V–I)$ colours among the individual constituents of each supercluster is typically $\sim$0.2–0.3 mag. Although some fraction of this spread could be attributed to the fact that superclusters are not really SSPs, it is nevertheless consistent with the scatter among different low-mass realizations of a true SSP. For example, using Monte Carlo simulations, Bruzual (2002) finds 3σ fluctuations in $(V–K)$ of almost 2 mag for a 1×10^4 $M_\odot$ cluster at a given age. Moreover, the distribution of $(V–I)$ colours of individual clusters within each supercluster looks reasonably Gaussian for all except supercluster SWB VII. There are only 12 star clusters type VII, and while the mode of the distribution (three clusters) lies around $(V–I) = 1$, there is a tail (two clusters) with $(V–I) > 1.4$. This tail could be produced by real population differences or, again, by small-number statistics.

3 STELLAR POPULATION MODEL PREDICTIONS

Central to this paper is the comparison between, on the one hand, the observed optical photometry and K_s-band fluctuation magnitudes of MC superclusters, and, on the other, the properties of synthetic single-age, single-metallicity stellar populations as predicted by BC03 and Mouhcine & Lançon (2003, hereafter ML03) stellar population synthesis models, respectively. BC03 models range from 0.1 Myr to 17 Gyr in age, while those of ML03 go from 12 Myr to 16 Gyr. Both sets of models span initial stellar metallicities of $Z/Z_\odot = 1/50$ to $Z/Z_\odot = 2.5$. Here, we describe briefly the main ingredients of the stellar population synthesis models, referring to the quoted papers for more details. Note that other sets of theoretical predictions of near-IR K_s-band SBF magnitudes and optical colours are published; however, they generally use BC03 isochrones or one of their earlier versions (Liu & Graham 2001; Mei et al. 2001), or they are computed for old stellar populations only, i.e. they do not cover the stellar population age range spanned by the MC superclusters (e.g. Worthey 1993a,b; Blakeslee et al. 2001; Cantiello et al. 2003).

[5] In the case of the two clusters for which only $F555W$ radial profiles (Mackey & Gilmore 2003) were available, integrated magnitudes were derived with diaphragms of 60 arcsec.

[6] When we change the input centre for the I photometry – we do not have V images – between 5 and 10 arcsec, the $(V–I)$ colour of a single cluster shifts by about 0.1 mag.

[7] The compilation by van den Bergh (1981) does not quote errors for the V photometry, but marks as uncertain $(U–B)$ or $(B–V)$ values for which any two observations differ by more than 0.1 mag. Among van den Bergh's sources, only van den Bergh & Hagen (1968) and Alcaino (1978) list errors for V. Hence, the clusters in our work with published errors go from 18 per cent for SWB class VI to 75 per cent for SWB type VII. For supercluster type VII, we have calculated the uncertainty in $(V–I)$ using the errors in these papers; it differs only by 0.01 mag from that derived with the procedure described above.

Table 2. *V* photometry sources different from van den Bergh (1981).

Supercluster	Name	Source
Pre-SWB	NGC 1727	Bica et al. (1996)
	NGC 1936 (IC 2127)	Bica et al. (1996)
	NGC 2014	Bica et al. (1996)
	NGC 2074	Bica et al. (1996)
	NGC 2001	Bica et al. (1996)
I	NGC 299	Alcaino (1978)
IV	SL 663	Mackey & Gilmore (2003)[a]
V	SL 363	Bernard & Bigay (1974); Bernard (1975); Bica et al. (1996)
	SL 556	Bica et al. (1996)
	SL 855	Mackey & Gilmore (2003)[a]
VI	SL 842	Bica et al. (1996)
	ESO 121-SC03	Mateo, Hodge & Schommer (1986)
VII	NGC 1786	van den Bergh (1981) and Bica et al. (1996)[b]

[a] *F555W* magnitudes were first obtained by integrating over the radial luminosity profiles published by Mackey & Gilmore (2003), then transformed to *V* with the relations of Dolphin (2000) (without charge transfer terms), assuming (*B*–*V*) colours from Elson & Fall (1985) appropriate for the *s* types (Elson & Fall 1988) of the clusters.
[b] van den Bergh (1981) lists $V = 10.88$ and states that only observations corrected for the contribution of a foreground star have been considered, but neglects giving a diaphragm. Bica et al. (1996) register both a *V* mag of 10.88 and a diaphragm of 60 arcsec.

Table 3. $\bar{M}_{K_s}$ and (*V*–*I*) values.

Supercluster	$\bar{M}_{K_s}$	(*V*–*I*)
Pre	-7.70 ± 0.40	0.34 ± 0.14
I	-8.85 ± 0.12	0.61 ± 0.08
II	-7.84 ± 0.28	0.48 ± 0.10
III	-7.45 ± 0.24	0.47 ± 0.06
IV	-7.51 ± 0.18	0.54 ± 0.05
V	-6.69 ± 0.20	0.78 ± 0.11
VI	-6.21 ± 0.24	1.02 ± 0.07
VII	-4.92 ± 0.38	1.06 ± 0.13

3.1 Single stellar population models

ML03 stellar population synthesis models were designed to reproduce the near-IR properties of both resolved and unresolved stellar populations, with an emphasis on intermediate-age stellar populations. The library of evolutionary tracks used by ML03 is based on the models of Bressan et al. (1993) and Fagotto et al. (1994a,b,c). We refer to these sets as the Padova tracks hereafter. The sets of tracks cover major stellar evolutionary phases: from the main sequence to the end of the early-AGB phase for low- and intermediate-mass stars, and to the central carbon ignition for massive stars. The Padova tracks do not extend to the end of the thermally pulsing AGB phase (TP-AGB hereafter). The high luminosities and low effective temperatures of stars evolving through this phase make them among the main contributors to the integrated near-IR light of stellar systems within the age interval when these stars are alive (e.g. Frogel et al. 1990; Mouhcine & Lançon 2002). The extension of these tracks to cover the TP-AGB phase is then needed. Until this happens, the evolution of low- and intermediate-mass stars through the TP-AGB evolutionary phase is followed using the so-called synthetic evolution modelling (e.g. Iben & Truran 1978; Renzini & Voli 1981; see also Marigo, Girardi & Chiosi 2003, for another attempt to include the TP-AGB in stellar population models). The complex interplay between different processes affecting stellar evolution through the TP-AGB phase are taken into account in the synthetic evolution models used by ML03. The properties of TP-AGB stars are allowed to evolve according to semi-analytical prescriptions. These prescriptions take into account the effect of metallicity on the instantaneous properties of TP-AGB stars. The evolution of TP-AGB stars is stopped at the end of the AGB phase, because their contribution to the optical/near-IR light is almost negligible once they evolve beyond this phase. The models predict the effective temperatures, bolometric luminosities, lifetimes and relative lifetimes of the carbon-rich phase of TP-AGB stars.

The BC03 models we compare to the observed properties of MC superclusters are those that these authors call the standard reference models. These models were built using isochrones based on Padova stellar evolutionary tracks. To extend the Padova low- and intermediate-mass stars beyond the early-AGB, BC03 adopt the effective temperature, bolometric luminosities and lifetimes of TP-AGB stars from Vassiliadis & Wood (1993). The relative lifetimes in the carbon-rich phase for TP-AGB stars were taken from Groenewegen & de Jong (1993) and Groenewegen, van den Hoek & de Jong (1995).

Stellar libraries are needed to assign spectral energy distributions to the stars of a synthetic population. For stars evolving through phases other than the TP-AGB, ML03 have used the theoretical stellar atmospheres of Kurucz (see Kurucz 1979), Fluks et al. (1994) and Bessell et al. (1989, 1991), as collected and recalibrated by Lejeune, Cuisinier & Buser (1997, 1998). BC03 use also the atmosphere compilations by Lejeune et al., as corrected by Westera (2001) and Westera et al. (2002). These stellar spectral libraries do not include spectra of TP-AGB stars. The spectrophotometric properties of TP-AGB stars are different from those of other cool and luminous stars. Their extended and cool atmospheres lead to the formation of deep and specific spectral absorption bands. On the other hand, the photometric properties of oxygen-rich and carbon-rich TP-AGB stars are different, i.e. as an example, carbon stars show redder (*H*–*K*) colours than oxygen-rich TP-AGB stars at a given (*J*–*H*) colour. To account for TP-AGB star properties, ML03 have used the empirical library of average TP-AGB oxygen-rich and carbon-rich star spectra of Lançon & Mouhcine (2002). The empirical average spectra of carbon stars from Lançon & Mouhcine (2002) are used at all metallicities. It is extremely difficult, however, to estimate the effective temperature and the metallicity of TP-AGB oxygen-rich stars;

instead, ML03 use a metallicity-dependent effective temperature scale (Bessell et al. 1991). To account for the spectral properties of carbon-rich TP-AGB stars, BC03 have constructed period-averaged spectra using solar metallicity model atmospheres for carbon stars from Höfner et al. (2000). These spectra were used to represent carbon stars of all metallicities in BC03 models.

K_s-band fluctuation magnitudes were computed from the models, as has been amply described in Paper I and summarized in Mouhcine et al. (2005). In this case, the second moment of the luminosity function is calculated by summing $L_{K_s}^2$ over all stellar types in the models; the integrated luminosity is obtained by summing the L_{K_s} of all types of star. Correspondingly, model (V–I) colours were constructed by summing the V and I fluxes of all the stars in the isochrones.

3.2 Comparison between models

Fig. 1 presents a comparison between the evolution of single-age, single-metallicity stellar population properties in the $\bar{M}_{K_s}$ versus (V–I) diagram as predicted by BC03 and ML03 stellar population synthesis models, respectively, for all the metallicities considered. The figure shows that both sets of models predict a qualitatively similar evolution over the age range comprised by them; i.e. the K_s-band SBF magnitudes become fainter as the (V–I) colour becomes redder. For both sets of stellar population model predictions, the (V–I) colour increases gradually to redder values as the stellar populations age. On the other hand, it is predicted by both BC03 and ML03 models that at a fixed age, single-age, single-metallicity stellar populations show redder (V–I) colours at higher metallicity. This is because, at fixed initial stellar mass, lowering metallicity causes stars to evolve at higher effective temperatures. In view of the monotonic and smooth evolution of the (V–I) colour, and given its weaker sensitivity (compared to the near-IR wavelength range) to the presence of very cool and luminous stars, this colour index can be regarded as a primary age indicator at fixed metallicity.

For the stellar populations dominated by red supergiant stars, i.e. younger than a few × 10 Myr, the K_s-band SBF magnitude becomes drastically fainter with age; on the other hand, the (V–I) changes by a modest factor around ∼0.3 mag. This trend is produced by the combination of two facts: (i) the masses, and hence the luminosities, of the red supergiant stars that drive the fluctuation signal change significantly, while (ii) the combined mass of main-sequence stars, which determine the integrated optical properties, remains almost constant.

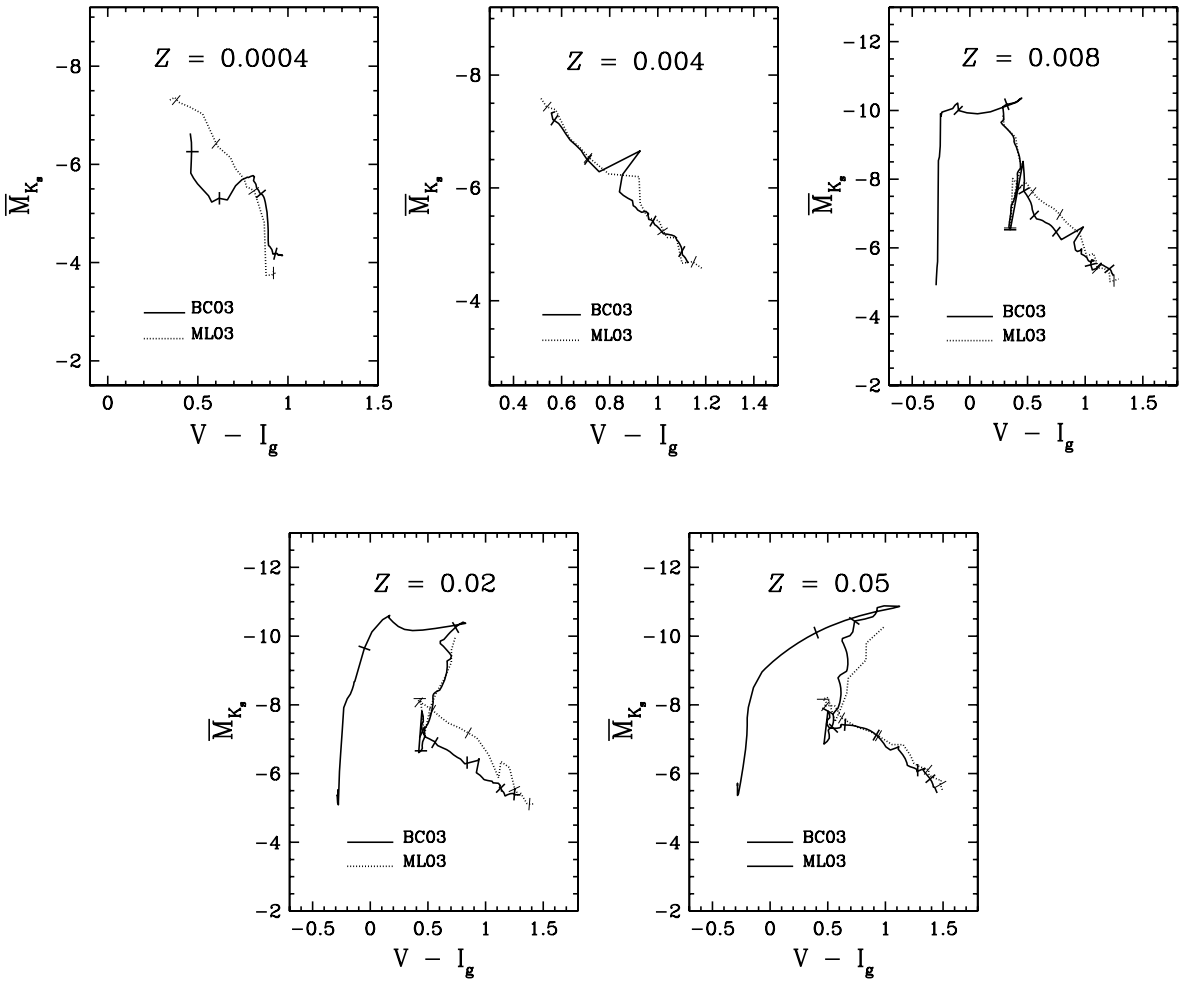

Figure 1. Comparison of model $\bar{M}_{K_s}$ versus (V–I_g) colour for $Z = 0.0004$ (top left), $Z = 0.004$ (top middle), $Z = 0.008$ (top right), $Z = 0.02$ (bottom left), and $Z = 0.05$ (bottom middle). Solid lines, BC03; dotted lines, ML03. For $Z = 0.0004$ and $Z = 0.004$, the evolution of models is shown only between ∼300 Myr and ∼16 Gyr. In the remaining panels, BC03 and ML03 models start at 2.4 and 12 Myr, respectively. From left to right, tick marks indicate 5 and 10 Myr (only for BC03, $Z \geqslant 0.008$ models), 100 and 200 Myr (for BC03 and ML03 models with $Z \geqslant 0.008$), 0.4, 1, 4 and 12 Gyr (all models).

When red supergiant stars disappear from a stellar population, AGB stars drive the evolution of the near-IR properties up to 1.5–2 Gyr. For populations dominated by short-lived massive AGB stars, i.e. younger than ∼200 Myr, the predicted evolution in the $\bar{M}_{K_s}$ versus $(V–I)$ diagram is complex. When the first (massive) AGB stars emerge in the stellar population, a brightening of the K_s-band SBF magnitude is predicted, at almost fixed $(V–I)$ colour. This is because of the overluminosity produced by the envelope burning that affects AGB stars with large initial stellar masses, i.e. $M_{\rm init} \gtrsim 3.5$–4 $M_\odot$ (see, for example, Mouhcine & Lançon 2002, for more details on the effects of envelope burning on intermediate-age stellar population properties). The observed counterparts of single-age, single-metallicity stellar populations within this age range are expected to cluster at the same location in the $\bar{M}_{K_s}$ versus $(V–I)$ diagram, i.e. in the region around $(V–I) \sim 0.4$ and $\bar{M}_{K_s} \sim -7.5$. During this age interval, the models have no ability for stellar population age dating and/or metallicity estimate.

For stellar populations older than ∼300 Myr, in which AGB stars are not affected by envelope burning, both sets of models predict a monotonic dimming of the K_s-band SBF magnitudes as the $(V–I)$ colour becomes redder. This evolutionary pattern continues for older stellar populations, i.e. older than 2–3 Gyr, when RGB stars drive their near-IR properties. This is because of the evolution of late-type giant star content. As a stellar population ages, the mass of the stars fuelling the evolution of near-IR properties, i.e. AGB stars for ages younger than ∼1.5 Gyr, and red giant stars for older ages, decreases. Consequently, at a fixed metallicity, the average luminosities of the AGB and RGB decrease with stellar population age. Conversely, at a fixed age, $\bar{M}_{K_s}$ magnitudes become brighter and the $(V–I)$ colour becomes redder as the stellar population metallicity increases. Thus, both the BC03 and ML03 sets of models predict that, as the metallicity increases, populations with the same age move to the upper right in the $\bar{M}_{K_s}$ versus $(V–I)$ diagram.

Despite the qualitative agreement between the BC03 and ML03 sets of theoretical predictions, differences between the two are apparent. At a given stellar metallicity, the evolutionary track in the $\bar{M}_{K_s}$ versus $(V–I)$ diagram predicted by ML03 models is systematically redder than that predicted by BC03 models. For stellar populations with $Z = 0.0004$, 0.008 and 0.02, and between ages 300 Myr and 1.5 Gyr, the models based on ML03 isochrones predict, at similar $(V–I)$ colours, brighter K_s-band SBF magnitudes (see also Mouhcine et al. 2005). Observationally, this means that for a given $(V–I)$ colour, models based on BC03 isochrones will attribute a higher metallicity to a star cluster with a certain $\bar{M}_{K_s}$ magnitude. The K_s-band SBF magnitude in the models based on ML03 isochrones is more sensitive to the presence of AGB stars. This is due to the fact that the AGB lifetimes used in the ML03 stellar population synthesis models are larger, thus increasing the contribution of these stars to the K_s-band light budget.

4 MODELS VERSUS OBSERVATIONAL DATA

Figs 2 and 3 show the comparison of $\bar{M}_{K_s}$ versus $(V–I_g)$ colour of MC superclusters with both sets of models. BC03 models are presented in the left-hand panels, while ML03 models are displayed on the right. Fig. 2 presents models with $Z = 0.0004$, 0.004 and 0.008. Even though the superclusters all have $Z \lesssim 0.01$, for completeness Fig. 3 illustrates the evolution of models with solar metallicity and $Z = 0.05$; the models with $Z = 0.008$ are also shown in Fig. 3, for comparison purposes. The solid dots represent the MC supercluster data, and the rectangle marks the general locus of the Liu et al. (2002) galaxy sample. The observed $(V–I_C)$ galaxy colours reported by Liu et al. were transformed to $(V–I_g)$, assuming that the mean stellar metallicities of the sample galaxies cover the range $0.008 < Z < 0.05$, by the following equation:

$$(V–I_g) = (1.050 \pm 0.006)(V–I_C) - (0.005 \pm 0.002). \quad (2)$$

Focusing first on the data and on Fig. 2, we notice that the youngest pre-SWB and SWB I superclusters, respectively at $(V–I) = 0.34$ and $(V–I) = 0.61$, are observed with significantly redder optical colours than predicted by the models with $Z = 0.008$, those closest to their metallicity of $Z = 0.01$ (Cohen 1982). Given their young ages, though, this is not surprising; Charlot & Fall (2000) offer the prescription that populations younger than $\sim 10^7$ yr suffer from about three times more reddening than later in their

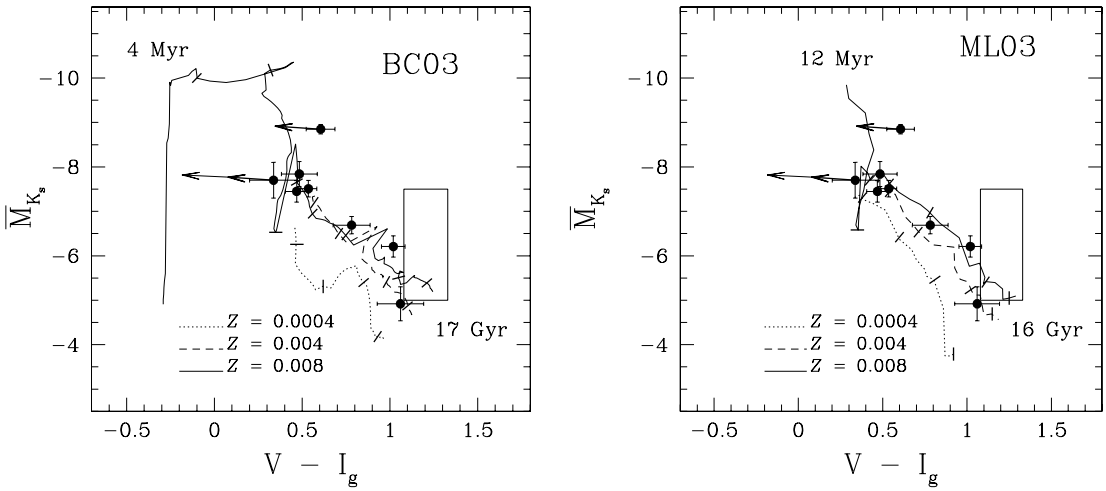

Figure 2. Comparison of $\bar{M}_{K_s}$ versus $(V–I_g)$ colour of MC superclusters with low-Z models by BC03 (left-hand panel) and by ML03 (right-hand panel). Dotted line, model with $Z = 0.0004$; dashed line, $Z = 0.004$; solid line, $Z = 0.008$. Tickmarks as in Fig. 1. The thick arrows deredden the pre-SWB and SWB I superclusters by $E(B–V) = 0.2$ above the average of the LMC. The thin arrow dereddens the pre-SWB supercluster by an additional $E(B–V) = 0.15$ (see text). The rectangle marks locus of the Liu et al. (2002) galaxy sample.

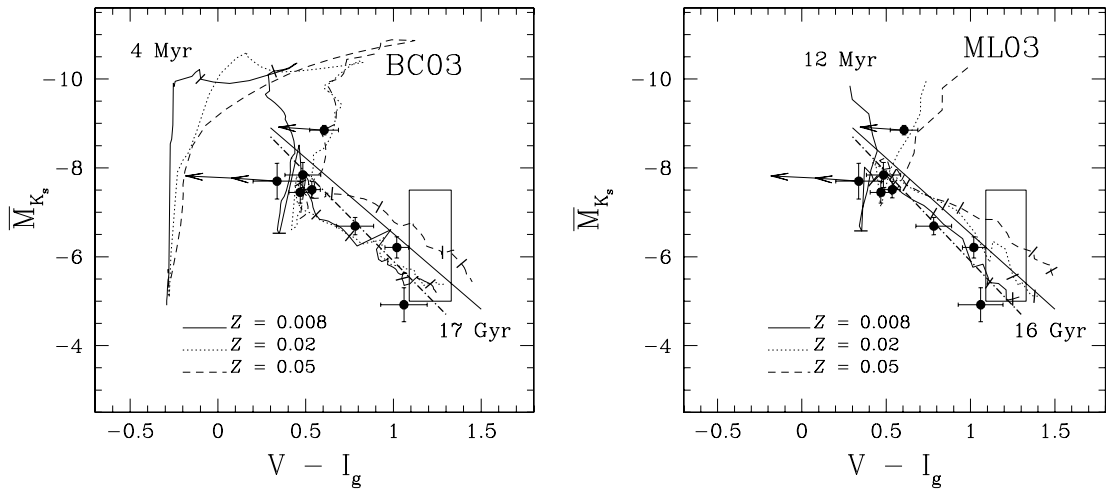

Figure 3. Comparison of $\bar{M}_{K_s}$ versus $(V–I_g)$ colour of MC superclusters with high-Z models by BC03 (left-hand panel) and by ML03 (right-hand panel). Solid line, model with $Z = 0.008$; dotted line, $Z = 0.02$; dashed line, $Z = 0.05$. Evolution before ∼300 Myr is now shown for all models. Symbols as in Figs 1 and 2, except that the BC03 model with $Z = 0.02$ is shown without tickmarks, because it runs so closely to the $Z = 0.008$ model. The straight solid line is best fit to the Liu et al. (2002) sample of early-type galaxies and spiral bulges. The straight dot-dashed line is our fit to superclusters I–VI (see text).

lifetimes.[8] Concordantly, for example, Grebel & Chu (2000) have measured a total colour excess (including foreground extinction) $E(B–V) = 0.28 \pm 0.05$ for Hodge 301, a relatively old cluster in 30 Dor for which these authors also derive an age of 20–25 Myr. This is the mean age of the star clusters that compose the supercluster type I (Paper I), if one adopts the age calibration by Elson & Fall (1985). Interestingly, if one dereddens the SWB I supercluster by an extra 0.20 mag in $E(B–V)$, or the difference between the measurement by Grebel & Chu (2000) and the average 0.08 mag that was adopted for the LMC (Schlegel et al. 1998), the data point falls exactly on the models with $Z = 0.008$. We follow a similar procedure for the pre-SWB supercluster. Both Parker (1993) and Dickel et al. (1994) have measured an average reddening of $E(B–V) \sim 0.43$ towards the whole of the 30 Dor region, while Selman et al. (1999) have determined a radially dependent reddening in the direction of R136 that reaches $E(B–V) \gtrsim 0.5$ at the centre of the cluster and declines to $E(B–V) \sim 0.3$ at $r = 1$ arcmin. Dereddening the youngest, pre-SWB supercluster by $E(B–V) = 0.35$ above the average of the LMC places it right where the BC03 models predict a population younger than 5 Myr should be in Figs 2 and 3. It is possible that the fluctuation magnitudes derived for the pre-SWB and type I superclusters suffer from a certain degree of crowding (Mouhcine et al. 2005). If this is the case, the correct values would be fainter than those reported, but would still lie along the same model sequence, at ages, respectively, slightly younger and slightly older. For the rest of the MC supercluster data points we attempt no further correction.

The evolution predicted by the models of the K_s-band SBF magnitudes as a function of the $(V–I)$ colour agrees remarkably well with the observed sequence defined by the MC superclusters. Superclusters of SWB types II, III and IV have ages of 35, 105 and 320 Myr, respectively, using the SWB class–age transformation of Frogel et al. (1990). Their observed loci concur well with the predicted location of stellar populations with ages between a few ×∼10 Myr and ∼300 Myr, in the region at $(V–I) \sim 0.4$ mag and $\bar{M}_{K_s} \sim -7.5$ mag. SWB types V, VI and VII correspond to ages of ∼1, 3 and 9 Gyr, respectively. For older stellar populations, the predicted monotonic fading of the K_s-band SBF magnitudes as the $(V–I)$ colour becomes redder agrees with the observed properties of intermediate-age and old MC superclusters.

However, one cannot fail to notice that the MC superclusters older than ∼3 Gyr (i.e. with SWB types VI and VII) are not very well matched by the models. Given their respective ages and metallicities,[9] the type VI supercluster mostly seems brighter in $\bar{M}_{K_s}$, while type VII mainly appears redder in $(V–I)$ than the model predictions. We remind the reader here that the measured $(V–I)$ colours could be slightly biased to the red as a consequence of our ignorance of the exact telescope pointings used for the acquisition of the V data (see Section 2.2). We have discussed in the same section that the colour distribution of the individual SWB VII clusters shows evidence of slight population differences, although we could also be seeing the effects of small-number statistics (12 clusters).

As advanced in Section 1, it is readily apparent in Figs 2 and 3 that the MC superclusters have greatly increased the range in $\bar{M}_{K_s}$ versus $(V–I)$ that is now accessible for exploration. We have plotted in both panels of Fig. 3, as a solid straight line, the linear fit found by Liu et al. (2002) to their early-type galaxy and spiral bulge data set. After transforming $(V–I_C)$ to $(V–I_g)$ with equation (2), this relation becomes

$$\bar{M}_{K_s} = (-5.84 \pm 0.04) + (3.4 \pm 0.8)[(V–I_g)_0 - 1.20]. \quad (3)$$

It is remarkable that, with the exception of the extremely young supercluster pre-SWB, and the old, metal-poor supercluster SWB class VII, the remaining MC superclusters lie roughly along the correlation found by Liu et al. (2002). In fact, a fit to superclusters I (corrected for extra extinction as explained in Section 4) through VI yields

$$\bar{M}_{K_s} = (-5.1 \pm 0.4) + (4.0 \pm 0.6)[(V–I_g)_0 - 1.20]. \quad (4)$$

This is also shown in Fig. 3, as a straight dot-dashed line. Within the errors, the relations for MC superclusters and galaxies,

[8] Exactly the same relation between age and reddening was found observationally by van den Bergh & Hagen (1968) for the MC clusters.

[9] For these SWB types, $0.002 \lesssim Z \lesssim 0.0008$ (Frogel et al. 1990).

respectively, have the same slope,[10] at the same time that the MC superclusters have a systematically lower $\bar{M}_{K_s}$ magnitude, at a fixed (V–I) colour, than what is predicted for early-type galaxies. The observed offset can be explained, according to both the BC03 and ML03 sets of models, as a metallicity effect. The metallicity of the MC superclusters in the fit is roughly (bar only SWB class VI) half that of the sample of early-type galaxies and spiral bulges. For a given (V–I) colour, the metal-poor simple stellar populations are on average older than the metal-rich ones, having then fainter $\bar{M}_{K_s}$ as a consequence of both lower metallicities and older ages.

We refer the reader to Paper I for a detailed discussion of the reasons for the monotonic decline of the K_s-band SBF brightness with age displayed by intermediate-age and old populations. When compared to both sets of models, the result obtained here for the MC superclusters backs the interpretation offered in Liu et al. (2002), that their galaxy sample constitutes a sequence. Namely, that objects with brighter SBFs have a more recent latest star formation burst (or a more extended star formation history), and that the most recent bursts in every object have all occurred at roughly constant metallicity. This is so because their sample lies on a straight line, parallel to the age sequence of their single metallicity models. Simultaneously, the fact that there exists a discernible offset between the galaxies and the MC superclusters confirms that the $\bar{M}_{K_s}$ versus (V–I) plane may contribute to the decoupling of age and metallicity effects in intermediate-age and old stellar systems. Particularly worthy of notice is the observation that the two samples offer consistent results, considering that galaxies are composite stellar systems, while the superclusters are approximately SSPs. The most likely explanation is that, being mostly probes of the brightest stars in a population at a given wavelength, SBFs are relatively insensitive to an underlying older population in composite systems.

It is also interesting to remark here that, while the BC03 models attribute a higher metallicity to NGC 1419 and 1389, the two Fornax objects left out of their fit (through sigma-clipping) by Liu et al. (2002), the ML03 model with solar metallicity (Fig. 3, right-hand panel, dotted line) shows an excursion to brighter SBF magnitudes at exactly the right place to ascribe to them the same metallicity as to other galaxies that do lie on the linear fit. This is a consequence of the longer lifetimes of TP-AGB stars in ML03 models. Hence, longer TP-AGB lifetimes could partly explain the observations of galaxies with $\bar{M}_{K_s}$ brighter than predicted, given their (V–I) colour.

Last but not least, we want to mention here that the largest sample to date of galaxies put together for SBF studies has been presented by Jensen et al. (2003). The 65 objects in this sample, however, were observed with the Near-IR Camera and Multi-Object Spectrometer (NICMOS) camera 2 (NIC2) on board the *Hubble Space Telescope* (*HST*), using the $F160W$ filter. The photometric transformation between the NIC2 and the commonly used near-IR ground-based filters is particularly difficult, for several reasons: the very deep molecular absorption bands in the star themselves; the significant differences between the *HST* and the ground-based filters; and the fact that telluric absorption features are very deep in ground-based observations but completely absent in data obtained from space (Stephens et al. 2000). Dealing with fluctuation magnitudes has an added degree of complexity, and conflicting statements can be found in the literature with regard to what colour to use to determine the correct transformation coefficients; i.e. the fluctuation colour of the population (Buzzoni 1993; Blakeslee et al. 2001), or the mean of the integrated and the fluctuation colours (Tonry et al. 1997). With all these caveats, we have transformed the relation between $\bar{M}_{F160W}$ and (V–I_C), derived by Jensen et al. (2003) from the 47 galaxies in their sample that show no signs of dust in the NIC2 field of view, into one between $\bar{M}_H$ and (V–I_g). To this end, we have relied on equation (2), and on the transformation between $\bar{M}_H$ and $\bar{M}_{F160W}$ obtained in equation (2) of Paper I.[11] For (J–K_s), we have substituted 0.92 $\pm$ 0.06, which is the average integrated colour of the mentioned 47 galaxies, as obtained from the 2MASS Extended Source Catalogue (XSC), via the GATOR catalogue query page. This is the result:

$$\bar{M}_H = (-5.12 \pm 0.09) + (4.9 \pm 0.5)[(V\text{–}I_g)_0 - 1.21]. \quad (5)$$

For the MC clusters, using the values for $\bar{M}_H$ derived in Paper I and in González et al. (2005), with the fluctuation magnitude for the supercluster type I once again corrected for extra extinction as in Section 4, the relation reads:

$$\bar{M}_H = (-4.0 \pm 0.5) + (4.8 \pm 0.7)[(V\text{–}I_g)_0 - 1.21]. \quad (6)$$

Even if tentative, because the near-IR observations of galaxies and star clusters have not been performed through the same filter, the conclusion is the same as that drawn from the K_s fluctuations: the slope for early-type galaxies and MC superclusters is the same within the errors; the MC clusters have fainter fluctuation magnitudes at a given (V–I_g) colour, as a result of their lower metallicity. It would certainly be worthwhile to obtain the data needed to perform a fairer comparison of galaxies and MC star clusters in the H observing window in the future. Table 4 lists the coefficients of our fits to the MC supercluster data; the reduced chi-square ($\widetilde{\chi}^2$) and the rms of the points (in magnitudes) after the fits are also included.

Table 4. Fluctuation absolute magnitude versus colour. Fits of the form $\bar{M} = a + b[(V\text{–}I_g)_0 -$ reference colour]; the number of objects used for the fit is tabulated as N. The resulting rms of the points (in magnitudes) after the fit and the reduced chi-square ($\widetilde{\chi}^2$) are also listed.

$\bar{M}$	a	b	N	rms	$\widetilde{\chi}^2$
$\bar{M}_{K_s}$	-5.1 ± 0.4	4.0 ± 0.6	6	0.85	1.02
$\bar{M}_H$	-4.0 ± 0.5	4.8 ± 0.7	6	1.04	1.28

5 SUMMARY AND CONCLUSIONS

In this paper we have presented the relation between absolute K_s-band SBF magnitude and (V–I) integrated colour for more than 180 MC star clusters. The newly reported results extend to fluctuation magnitudes $\bar{M}_{K_s} \sim -9$ and optical colour (V–I) ~ -0.4 the linear relation observed already for early-type galaxies and spiral galaxy bulges in a more limited range of both fluctuation magnitudes and colour [$-5 \gtrsim \bar{M}_{K_s} \gtrsim -7$, $1.0 \lesssim (V\text{–}I) \lesssim 1.25$].

This empirical relation has been compared to the predicted evolution of single-age, single-metallicity stellar population properties in the $\bar{M}_{K_s}$ versus (V–I) diagram, based on both BC03 and ML03 isochrones. The predicted evolution and the observed sequence agree quite well over the ranges of $\bar{M}_{K_s}$ magnitude and (V–I) colour covered by the data [$-5 \gtrsim \bar{M}_{K_s} \gtrsim -9$, $-0.4 \lesssim (V\text{–}I) \lesssim 1.25$]. With the exception of the extremely young supercluster pre-SWB, and possibly the old and metal-poor supercluster class VII, the remaining superclusters lie on the linear correlation already found

[10] If in fact the fluctuation magnitude of supercluster type I is affected by crowding and its true value is a few tenths of a mag dimmer, the match between the two slopes would be even better.

[11] $\bar{M}_H = \bar{M}_{F160W} + (0.08 \pm 0.07) - (0.24 \pm 0.05)\,(J\text{–}K_s + 0.48)$.

by Liu et al. (2002). Such correlation is observed in the ranges $-5 \gtrsim \bar{M}_{K_s} \gtrsim -9$, $0.3 \lesssim (V-I) \lesssim 1.25$. The existence of a linear correlation implies that star clusters, early-type galaxies and spiral bulges represent an age sequence, where younger stellar populations display brighter K_s-band SBF magnitudes and bluer $(V–I)$ colour. At the same time, the discernible offset between galaxies and MC star clusters confirms that the $\bar{M}_{K_s}$ versus $(V–I)$ plane may contribute to distinguish the effects of age and metallicity in intermediate-age and old stellar systems. One other suggestive result that emerges from the comparison between the galaxy sample and the models is that longer lifetimes of TP-AGB stars might partly explain galaxies with near-IR SBFs that are brighter than anticipated, given their $(V–I)$ colour. A preliminary comparison between the H 2MASS data of the MC star clusters and the sample of 47 early-type galaxies and spiral bulges observed by Jensen et al. (2003) through the $F160W$ filter leads to the same basic conclusions: galaxies and star clusters lie along correlations with the same slope, and there is a slight offset between the star cluster sample and the galaxies, caused by their different metallicities.

We have found that results from star clusters in the MC (i.e. SSPs in Local Group irregular and consequently relatively metal-poor galaxies) agree with those of spiral bulges and early-type galaxies (i.e. composite systems with higher metallicities than the MC), located not only in the Local Group, but also in mildly dense clusters of galaxies such as Fornax and Virgo. The implication is that the relationship between $\bar{M}_{K_s}$ and $(V–I)$ might be a fairly robust tool, rather insensitive to environment, at least in the local Universe, for the study of ages and metallicities of unresolved stellar populations, could provide additional constraints on star formation histories, and aid in the calibration of the K_s-band SBFs for cosmological distance measurements. In this regard – the determination of cosmological distances – the sensitivity of near-IR SBFs to stellar ages and metallicities, and perhaps to the details of AGB evolution in intermediate-age populations, is a potential caveat to bear in mind, albeit not necessarily in the local Universe or in view of today's observing capabilities. For example, Ferreras, Charlot & Silk (1999) have analysed early-type galaxies in Coma and 17 clusters at $0.3 \lesssim z \lesssim 0.9$; their results imply that only galaxies smaller than $0.5\,L_*$, at redshifts $z \gtrsim 0.5$, can be expected to harbour populations with metallicities below solar.

ACKNOWLEDGMENTS

We thank the whole DENIS Team, especially G. Simon and its PI, N. Epchtein, for making available the DENIS data. The DENIS project is supported, in France by the Institut National des Sciences de l'Univers, the Education Ministry and the Centre National de la Recherche Scientifique, in Germany by the State of Baden Würtemberg, in Spain by the DGICYT, in Italy by the Consiglio Nazionale delle Ricerche, in Austria by the Fonds zur Förderung der wissenschaftlichen Forschung and the Bundesministerium für Wissenschaft und Forschung. RAG and MA acknowledge L. Carigi and A. Bressan for their very useful comments on the manuscript. We thank the referee, Joseph B. Jensen, for his careful reading of the paper; we are grateful for his suggestions.

REFERENCES

Ajhar E. A., Tonry J. L., 1994, ApJ, 429, 557
Alcaino G., 1978, A&AS, 34, 431
Bernard A., 1975, A&A, 40, 199
Bernard A., Bigay J. H., 1974, A&A, 33, 123
Bessell M. S., 1979, PASP, 91, 589
Bessell M. S., Brett J. M., Wood P. R., Scholz M., 1989, A&AS, 77, 1
Bessell M. S., Brett J. M., Scholz M., Wood P. R., 1991, A&AS, 89, 335
Bica E., Claria J. J., Dottori H., Santos J. F. C., Piatti A. E., 1996, ApJSS, 102, 57
Blakeslee J. P., Vazdekis A., Ajhar E. A., 2001, MNRAS, 320, 193
Bressan A., Fagotto F., Bertelli G., Chiosi C., 1993, A&AS, 100, 647
Bruzual A. G., 2002, in Geisler D., Grebel E. K., Minniti D., eds, Proc. IAU Symp. Vol. 207, Extragalactic Star Clusters. Astron. Soc. Pac., San Francisco, p. 616
Bruzual G., Charlot S., 2003, MNRAS, 344, 1000 (BC03)
Buzzoni A., 1989, ApJSS, 71, 817
Buzzoni A., 1993, A&A, 275, 433
Cantiello M., Raimondo G., Brocato E., Capaccioli M., 2003, AJ, 125, 2783
Cerviño M., Valls-Gabaud D., 2003, MNRAS, 338, 481
Cerviño M., Valls-Gabaud D., Luridiana V., Mas-Hesse J. M., 2002, A&A, 381, 51
Charlot S., Fall S. M., 2000, ApJ, 539, 718
Cioni M.-R. et al., 2000, A&AS, 144, 235
Cohen J. G., 1982, ApJ, 258, 143
Dickel J. R., Milne, D. K., Kennicutt R. C., Chu Y., Schommer R. A., 1994, AJ, 107, 1067
Dolphin A. E., 2000, PASP, 112, 1397
Elson R. A. W., Fall S. M., 1985, ApJ, 299, 211
Elson R. A. W., Fall S. M., 1988, AJ, 96, 1383
Epchtein N. et al., 1997, The Messenger, 87, 27
Fagotto F., Bressan A., Bertelli G., Chiosi C., 1994a, A&AS, 104, 365
Fagotto F., Bressan A., Bertelli G., Chiosi C., 1994b, A&AS, 105, 29
Fagotto F., Bressan A., Bertelli G., Chiosi C., 1994c, A&AS, 105, 39
Ferrarese L. et al., 2000, ApJSS, 128, 431
Ferreras I., Charlot, S., Silk J., 1999, ApJ, 521, 81
Fluks M. A., Plez B., Thé P. S., de Winter D., Westerlund B. E., Steenman H. C., 1994, A&AS, 105, 311
Fouqué P. et al., 2000, A&AS, 141, 313
Frogel J. A., Mould, J., Blanco V. M., 1990, ApJ, 352, 96
González R. A., Liu M. C., Bruzual G., 2004, ApJ, 611, 270 (Paper I)
González R. A., Liu M. C., Bruzual G., 2005, ApJ, 621, 557
Grebel E. K., Chu, Y., 2000, AJ, 119, 787
Groenewegen M., de Jong T., 1993, A&A, 267, 410
Groenewegen M., van den Hoek L. B., de Jong T., 1995, A&A, 293, 381
Höfner S., Loidl R., Aringer B., Jorgensen U. G., Hron J., 2000, in Salama A., Kessler M. F., Leech K., Schulz B., eds, ISO Beyond the Peaks: Proc. 2nd ISO Workshop on Analytical Spectroscopy. ESA-SP 456, p. 299
Iben I., Truran J. W., 1978, ApJ, 220, 980
Jensen J. B., Tonry J. L., Luppino G. A., 1998, ApJ, 505, 111
Jensen J. B., Tonry J. L., Thompson R. I., Ajhar E. A., Lauer T. R., Rieke M. J., Postman, M., Liu M. C., 2001, ApJ, 550, 503
Jensen J. B., Tonry J. L., Barris B. J., Thompson R. I., Liu M. C., Rieke M. J., Ajhar E. A., Blakeslee J. P., 2003, ApJ, 583, 712
Kurucz R. L., 1979, ApJS, 40, 1
Lançon A., Mouhcine M., 2002, A&A, 393, 167
Lejeune T., Cuisinier F., Buser R., 1997, A&AS, 125, 229
Lejeune T., Cuisinier F., Buser R., 1998, A&AS, 130, 65
Liu M. C., Graham J. R., 2001, ApJ, 557, L31
Liu M. C., Charlot S., Graham J. R., 2000, ApJ, 543, 644
Liu M. C., Graham J. R., Charlot S., 2002, ApJ, 564, 216
Mackey A. D., Gilmore G. F., 2003, MNRAS, 338, 85
Marigo P., Girardi L., Chiosi C., 2003, A&A, 403, 225
Mateo M., Hodge P., Schommer R. A., 1986, ApJ, 311, 113
Mei S., Quinn P. J., Silva D. R., 2001, A&A, 371, 779
Mouhcine, M., Lançon A., 2002, A&A, 393, 149
Mouhcine, M., Lançon A., 2003, A&A, 402, 425 (ML03)
Mouhcine M., González R. A., Liu M. C., 2005, MNRAS, 362, 1208
Parker J. W., 1993, AJ, 106, 560
Paturel G., Petit C., Rousseau J., Vauglin I., 2003, A&A, 405, 1
Renzini A., Voli M., 1981, A&A, 94, 175
Santos J. F. C., Frogel J. A., 1997, ApJ, 479, 764
Schlegel D. J., Finkbeiner D. P., Davis M., 1998, ApJ, 500, 525

Searle L., Wilkinson A., Bagnuolo W. G., 1980, ApJ, 239, 803
Selman F., Melnick J., Bosch G., Terlevich R., 1999, A&A, 341, 98
Skrutskie M. F. et al., 1997, in ASSL Vol. 210, The Impact of Large Scale Near-IR Sky Surveys. Kluwer, Dordrecht, p. 25
Stephens A. W., Frogel J. A., Ortolani S., Davies R., Jablonka P., Renzini A., Rich R. M., 2000, AJ, 119, 419
Tonry J., Schneider D. P., 1988, AJ, 96, 807
Tonry J. L., Ajhar, E. A., Luppino G. A., 1990, AJ, 100, 1416
Tonry J. L., Blakeslee J. P., Ajhar E. A., Dressler A., 1997, ApJ, 475, 399
van den Bergh S., 1981, A&AS, 46, 79
van den Bergh S., Hagen G. L., 1968, AJ, 73, 569
Vassiliadis E., Wood P. R., 1993, ApJ, 413, 641
Vazdekis A., Casuso, E., Peletier R. F., Beckman J. E., 1996, ApJSS, 106, 307
Westera P., 2001, PhD thesis, Univ. Basel
Westera P., Lejeune T., Buser R., Cuisinier F., Bruzual G., 2002, A&A, 381, 524
Worthey G., 1993a, ApJ, 409, 530
Worthey G., 1993b, ApJ, 418, 947

APPENDIX A: POPULATION VARIATIONS OR STOCHASTIC EFFECTS?

It is beyond the scope of the present paper to investigate in depth the role of stochastic effects in the integrated properties of stellar populations. However, for illustration purposes, we show in Fig. A1 the colour–magnitude diagrams (CMDs) of superclusters type IV (left-hand panel) and VI (right-hand panel). Fig. A2 is a copy of the right-hand panel of Fig. 2, this time indicating the locations of individual clusters types IV (open triangles) and VI (open circles) in the $\bar{M}_{K_s}$ versus $(V–I)$ plane. There are several facts worth noticing. First, the CMDs, narrow at the top and wide at the bottom, resemble more those of SSPs with 'normal' photometric errors than CMDs of composite populations (Bressan, private communication). This notwithstanding, and even when the relative offset between the general loci of the two SWB classes is clearly discernible, single clusters of each SWB type show a large scatter,[12] especially in fluctuation magnitude, which is determined by many fewer stars than the integrated colour. Taken together, the relatively narrow RGB and AGB, and the very large scatter of individual clusters in the $\bar{M}_{K_s}$ versus $(V–I)$ plane support the interpretation that stochastic effects might be more important than actual population variations in determining the integrated properties of single clusters within each SWB class. If this is the case, the construction of superclusters is an appropriate strategy to simulate more massive SSPs.

[12] On the basis of this plot alone, it could be argued that perhaps SL 663, at $(V–I) \sim 1.7$, does not belong in class SWB IV. Removing it leaves the fluctuation magnitude and integrated colour of supercluster type IV the same, within the quoted errors.

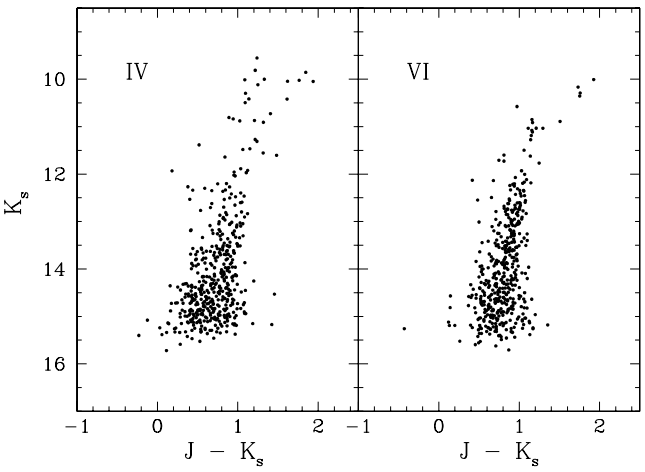

Figure A1. CMDs of MC superclusters types SWB IV (left-hand panel) and SWB VI (right-hand panel). Stars within 60 arcsec from the centre (at the distance of the LMC). Average photometric errors are 0.04 mag in brightness and 0.02 mag in colour for sources with $K_s \leqslant 13$; 0.06 and 0.03 mag for stars with $13 < K_s \leqslant 14$; and 0.13 and 0.07 mag (about the size of the dots) for sources with $14 < K_s \leqslant 15$.

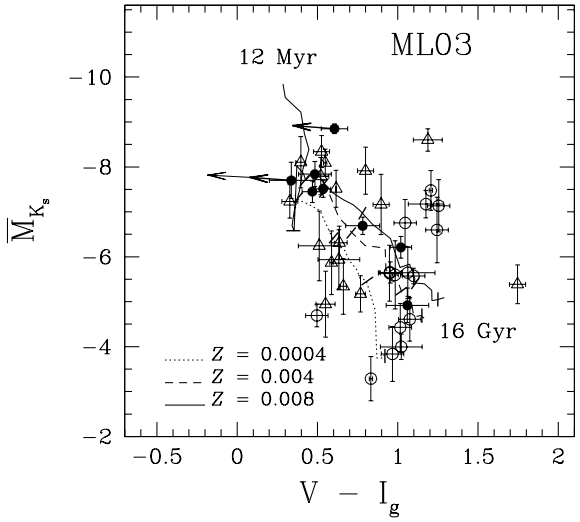

Figure A2. $\bar{M}_{K_s}$ versus $(V–I_g)$ colour of individual clusters classes SWB IV (open triangles) and SWB VI (open circles); all other symbols as in right-hand panel of Fig. 2.

This paper has been typeset from a TEX/LATEX file prepared by the author.